Spatial Quantum Signatures in Parametric Down-Conversion

I. Marzoli,* A. Gatti, and L. A. Lugiato

Istituto Nazionale per la Fisica della Materia, Dipartimento di Fisica dell'Università, via Celoria 16, I-20133 Milano, Italy

(Received 4 November 1996)

We calculate the normal and time ordered spatial intensity correlation function of the signal field in a degenerate parametric oscillator below threshold, with spherical mirrors. In the far field, it exhibits a two peak structure, and the correlation is maximal between points opposite each other with respect to the axis of the system. This feature provides direct spatial evidence of the twin photon emission, and identifies states of the radiated field with local nonclassical squeezing properties. [S0031-9007(97)02726-9]

PACS numbers: 42.50.Dv, 42.65.–k

The fundamental character of the twin photon emission in parametric down-conversion is well known. The pump photons are split into pairs of photons called signal and idler that are highly correlated both in time [1] and in photon number [2,3], and can be entangled in polarization [4]. The quadrature phase amplitudes of the signal and idler beams shown an Einstein-Podolsky-Rosen (EPR) paradox for continuous variables [5]. All these features exhibit in the best way the particle aspect of electromagnetic radiation, and are of quantum nature.

The aim of this article is to identify some prominent spatial aspects in the twin photon emission. We consider a degenerate optical parametric oscillator (OPO), with spherical mirrors. Below threshold, the signal field is purely generated by quantum fluctuations. The average intensity distribution corresponds to a wide spot with rotational symmetry, which does not show any corpuscular aspect. However, our recent analyses of quantum images [6,7] have shown that a spatial correlation function is able to reveal structures where the average intensity distribution is structureless.

The spatial intensity correlation function in the OPO below threshold has been calculated in [7] for the near field. However, the particle aspects emerge only in the far field [8]; as we show in this paper, the examination of the spatial correlation function of the intensity in the far field allows one to find the spatial quantum signature we are looking for.

A coherent and stationary field E_P, of frequency $2\omega_s$, is injected in a cavity (Fig. 1) with spherical and quasiplanar mirrors (i.e., the Rayleigh range of the cavity is much larger than the cavity length). E_P has a plane wave configuration (it is not reflected by the cavity mirrors) and, due to the intracavity medium with a $\chi^{(2)}$ nonlinearity, via parametric down-conversion generates a signal field A of frequency ω_s. Mirror M_2 is totally reflecting, and the input/output mirror M_1 has a high reflectivity for the signal field, with respect to which the cavity supports the Gauss-Laguerre modes [9]

$$f_{pli}(r,\varphi,z) = \tilde{f}_{pl}(r,z)e^{i[(z/z_0)[r^2/w(z)^2]-\theta_{pl}(z)]} \times \begin{cases} \cos(l\varphi), & i = 1\,, \\ \sin(l\varphi), & i = 2\,, \end{cases}$$

$$\tilde{f}_{pl}(r,z) = \frac{2}{w(z)\,(2^{\delta_{l,0}}\pi)^{1/2}}\sqrt{\frac{p!}{(p+l)!}}\left[\frac{2r^2}{w(z)^2}\right]^{l/2} \times L_p^l\left(\frac{2r^2}{w(z)^2}\right)e^{-r^2/w(z)^2},$$

where $p, l = 0, 1, 2, \ldots$,

$$w(z) = w_0\sqrt{1 + (z/z_0)^2}\,, \qquad z_0 = \pi w_0^2/\lambda\,, \quad (1)$$

$$\theta_{pl} = (2p + l + 1)tg^{-1}(z/z_0)\,, \quad (2)$$

z is the longitudinal coordinate (Fig. 1), $r = \sqrt{x^2 + y^2}$, φ is the angular coordinate in the transverse plane, w_0 and z_0 denote the beam waist and the Rayleigh range, respectively, and λ is the wavelength; L_p^l is the Laguerre polynomial of indicated indices. The mode frequencies are given by

$$\omega_{pl} = \omega_{00} + (2p + l)\eta\,, \quad (3)$$

where the intermode frequency spacing η depends on the curvature of the mirrors and on their distance [9]; modes with the same value of $2p + l$ are frequency degenerate. We use a single longitudinal mode model [6,7] formulated in the paraxial and mean field approximations, in which the intracavity signal field $A(\vec{x}, t)$, with $\vec{x} = (x, y)$, is independent of z and can be expanded as follows:

$$A(\vec{x},t) = A(r,\varphi,t) = \sum_{p,l,i} a_{pli}(t) f_{pli}(r,\varphi,z=0)\,, \quad (4)$$

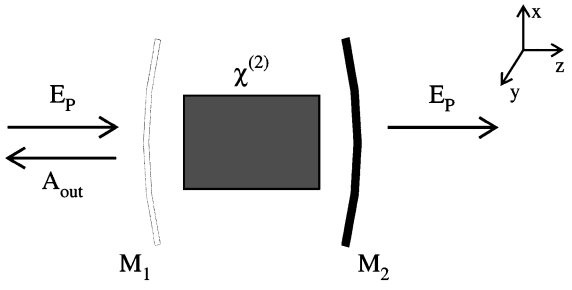

FIG. 1. Scheme of the system; A_{out} is the signal field.

 0031-9007/97/78(11)/2092(4)$10.00

where $a_{pli}, a^{\dagger}_{pli}$ are the annihilation and creation operators of photons which obey the commutation rule $[a_{pli}(t), a^{\dagger}_{p'l'i'}(t)] = \delta_{p,p'}\delta_{l,l'}\delta_{i,i'}$. Neglecting pump depletion, as it is legitimate below threshold, the density operator ρ of the signal field obeys the master equation in the interaction picture [6,7]:

$$\frac{d\rho}{dt} = \frac{1}{i\hbar}[H,\rho] + \sum_{p,l,i}\Lambda_{pli}\rho\,, \tag{5}$$

where the decay terms,

$$\Lambda_{pli}\rho = \gamma(2a_{pli}\rho a^{\dagger}_{pli} - \rho a^{\dagger}_{pli}a_{pli} - a^{\dagger}_{pli}a_{pli}\rho)\,, \tag{6}$$

contain the damping rate γ of the signal field, and the Hamiltonian is given by

$$H = H_{\rm free} + H_{\rm int}\,, \tag{7}$$

with

$$H_{\rm free} = \hbar\sum_{p,l,i}(\omega_{pli} - \omega_s)a^{\dagger}_{pli}a_{pli}\,, \tag{8}$$

$$H_{\rm int} = \frac{i\hbar\gamma}{2}\mathcal{A}_p\sum_{p,l,i}[(a^{\dagger}_{pli})^2 - a^2_{pli}], \tag{9}$$

and $\mathcal{A}_P = gE_P/\gamma$, where g is the coupling constant, proportional to the susceptibility $\chi^{(2)}$, and E_P is the amplitude of the pump field, treated as a real number.

In the following, we will consider three quantities which refer to the signal field out of the cavity $A_{\rm out}$; they are (1) the average intensity distribution $\langle I(\vec{x},z,t)\rangle$, with

$$I(\vec{x},z,t) = A^{\dagger}_{\rm out}(\vec{x},z,t)A_{\rm out}(\vec{x},z,t)\,. \tag{10}$$

By taking into account the input-output relation of the cavity [10], one obtains

$$\langle I(\vec{x},z,t)\rangle = \gamma\sum_{p,l}[\tilde{f}_{pl}(r,z)]^2\frac{\mathcal{A}_P^2}{1 - \mathcal{A}_P^2 + \Delta_{pl}^2}\,, \tag{11}$$

where $\Delta_{pl} = (\omega_{pl} - \omega_s)/\gamma$. (2) The space-time intensity correlation function

$$G(\vec{x},z,t;\vec{x}',z,t') = \langle ::\delta I(\vec{x},z,t)\delta I(\vec{x}',z,t'):: \rangle\,, \tag{12}$$

where $\delta I(\vec{x},z,t) = I(\vec{x},z,t) - \langle I(\vec{x},z,t)\rangle$, and :: :: denotes normal and time ordering. The explicit expression of G turns out to be

$$G(\vec{x},z,\tau;\vec{x}',z,0) = \gamma^2\mathcal{A}_P^2 e^{-2|\tau|}\Bigg\{\Bigg|\sum_{p,l}\frac{\tilde{f}_{pl}(r,z)\tilde{f}_{pl}(r',z)\cos[l(\varphi - \varphi')]}{1 - \mathcal{A}_P^2 + \Delta_{pl}^2} \times e^{2i\theta_{pl}(z)}\Bigg[\frac{\beta_{pl}}{\delta_{pl}}\sinh(\delta_{pl}|\tau|) + \alpha_{pl}\cosh(\delta_{pl}|\tau|)\Bigg]\Bigg|^2 + \mathcal{A}_P^2\Bigg[\sum_{pl}\frac{\tilde{f}_{pl}(r,z)\tilde{f}_{pl}(r',z)\cos[l(\varphi - \varphi')]}{1 - \mathcal{A}_P^2 + \Delta_{pl}^2}\Bigg(\frac{\sinh(\delta_{pl}|\tau|)}{\delta_{pl}} + \cosh(\delta_{pl}|\tau|)\Bigg)\Bigg]^2\Bigg\}, \tag{13}$$

where $\tau = \gamma t$, $\alpha_{pl} = 1 + i\Delta_{pl}$, $\beta_{pl} = \mathcal{A}_P^2 - \Delta_{pl}^2 + i\Delta_{pl}$, $\delta_{pl} = \sqrt{\mathcal{A}_P^2 - \Delta_{pl}^2}$. (3) The spectrum of the spatial intensity correlation function

$$\tilde{G}(\vec{x},z;\vec{x}',z;\omega) = \int_{-\infty}^{+\infty}dt e^{-i\omega t}G(\vec{x},z,t;\vec{x}',z,0)\,. \tag{14}$$

All the averages are calculated in the stationary state of the degenerate OPO below threshold. Because of translational symmetry in time, the average (10) does not depend on t, and G depends only on $(t - t')$; due to rotational symmetry, G and $\tilde{G}$ depend only on $\varphi - \varphi'$.

The mean intensity distribution, shown in Fig. 2(a), corresponds to a wide spot with cylindrical symmetry. When plotted as a function of the scaled transverse coordinates $x/w(z), y/w(z)$, it is independent of z; the same holds true for the correlation function when the OPO is below but close to threshold, because the dominant contribution to G arises from the frequency degenerate family of modes which is closest to resonance with the signal field frequency ω_s [7], and the propagation phase shift $\theta_{pl}(z)$ [see Eq. (2)] is the same for all these modes.

The interesting case is when the OPO is below threshold enough, so that G is built up by the contribution of several families of Gauss-Laguerre modes. In Figs. 2 and 3, scaled versions of G and $\tilde{G}$ are plotted as a function of $\vec{x}'/w(z)$, keeping the first point $\vec{x}$ fixed.

Figures 2(b) and 2(c) display the equal time correlation function $G(\vec{x},z,t;\vec{x}',z,t)$ in the near field and in the far field, respectively. The first one is peaked at $\vec{x}' = \vec{x}$, which is the standard configuration for a spatial correlation function. On the other hand, the far field configuration exhibits a dominant peak for $\vec{x}' = -\vec{x}$, i.e., when the two points are opposite to each other with respect to the axis of the system. This feature can be easily linked to the circumstance that, since Eqs. (5)–(9) describe a Gaussian stochastic process, one has

$$G(\vec{x},z,t;\vec{x}',z,t) = \langle A^{\dagger}_{\rm out}(\vec{x},z,t)A^{\dagger}_{\rm out}(\vec{x}',z,t)\rangle \times \langle A_{\rm out}(\vec{x}',z,t)A_{\rm out}(\vec{x},z,t)\rangle + \langle A^{\dagger}_{\rm out}(\vec{x},z,t)A_{\rm out}(\vec{x}',z,t)\rangle \times \langle A^{\dagger}_{\rm out}(\vec{x}',z,t)A_{\rm out}(\vec{x},z,t)\rangle\,, \tag{15}$$

where the two contributions correspond to the two parts at the right-hand side of Eq. (13) for $\tau = 0$, respectively. The second one is phase insensitive and is independent of z when expressed as a function of $\vec{x}/w(z)$. The first, phase-sensitive contribution arises from the two photon

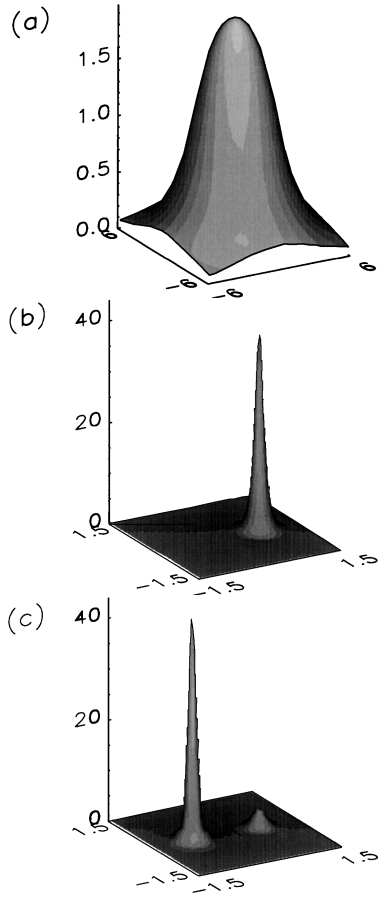

FIG. 2. (a) Average intensity distribution of the signal field for $\eta/\gamma = 0.1$, $\Delta_{00} = -0.5$, $\mathcal{A}_P = 0.5$. (b), (c) Equal time spatial intensity correlation function $Gw(z)^4/\gamma^2$ [see Eq. (12)] for the same parameters as in (a), and (b) $z/z_0 \ll 1$, (c) $z/z_0 = 200$.

character of the interaction and is dominant over the second. It corresponds to a peak for $\vec{x}' = \vec{x}$ in the near field, which is exactly shifted to the opposite side when $z/z_0 \to \infty$. For $\eta/\gamma \lesssim 1$, the qualitative shape shown in Figs. 2(b) and 2(c) is independent of the position $\vec{x}$ and of the values of Δ_{00} and $\mathcal{A}_P$ (provided that the OPO is not too close to the threshold region).

The spectrum $\tilde{G}(\vec{x}, z; \vec{x}', z; \omega)$ of the spatial correlation function exhibits qualitatively the same behavior as G; Fig. 3 shows how $\tilde{G}$ changes when z varies from the near to the far field. In comparison with G, the peaks are less narrow and, in the far field, the difference between the sizes of the autocorrelation peak ($\vec{x}' = \vec{x}$) and the anticorrelation peak ($\vec{x}' = -\vec{x}$) is smaller.

The emergence of the peak at $\vec{x}' = -\vec{x}$ is linked to the fact that the far field shows the particle aspect of radiation [8]. As shown by Fig. 2(a), there is no privileged direction of emission for the photons of the signal field. However they are emitted as pairs of twin photons: If a photon is emitted in the direction a in Fig. 4(a), a twin photon is emitted in the direction b in order to preserve the transverse momentum; hence maximum correlation with point a is shown by point b. This is the physical interpretation of the

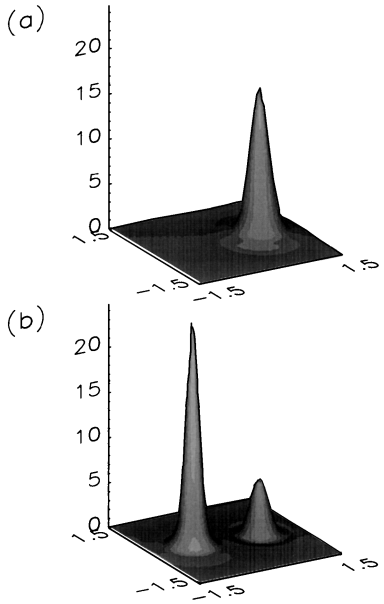

FIG. 3. Temporal Fourier transform $\tilde{G}w(z)^4/\gamma$ [see Eq. (13)] of the spatiotemporal intensity correlation function for $\omega = 0$, $\eta/\gamma = 0.1$, $\Delta_{00} = -0.5$, $\mathcal{A}_P = 0.5$; (a) $z/z_0 \ll 1$, (b) $z/z_0 = 40$.

structure of the spatial correlation function in the far field, which provides the spatial signature of the signal-idler correlation we were searching for. Next, we demonstrate that this two peak structure, with the peak at $\vec{x}' = -\vec{x}$ higher than the peak at $\vec{x}' = \vec{x}$, is a *quantum effect.* To this aim, let us consider two symmetrical regions $R(\vec{x})$ and $R(-\vec{x})$ centered at the two points $\vec{x}$ and $-\vec{x}$, respectively, and the difference between the number of photons collected in the two regions during the time interval Δt, i.e.,

$$\Delta I(\vec{x}, z) = \int_0^{\Delta t} dt I_-(\vec{x}, z, t)\,, \tag{16}$$

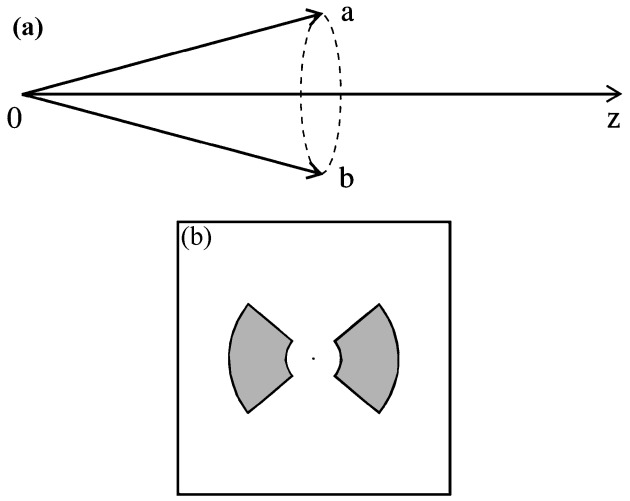

FIG. 4. (a) Twin photon emission in the OPO. (b) Shape of the regions $R(\vec{x})$ and $R(-\vec{x})$.

$$I_-(\vec{x},z,t) = \left\{ \int_{R(\vec{x})} d^2\vec{x}' - \int_{R(-\vec{x})} d^2\vec{x}' \right\} \times A^\dagger_{\rm out}(\vec{x}',z,t) A_{\rm out}(\vec{x}',z,t)\,. \quad (17)$$

Because of symmetry, $\langle \Delta I \rangle = 0$ but, due to quantum fluctuations, $\langle \Delta I^2 \rangle \neq 0$. For $\gamma \Delta t \ll 1$, and when the regions $R(\vec{x})$ and $R(-\vec{x})$ are so small that the integrand is nearly constant over each of them, calling σ the area of $R(\vec{x})$, one has

$$\langle \Delta I^2(\vec{x},z) \rangle = 2\{\Delta t \sigma \langle I(\vec{x},z,0)\rangle + \Delta t^2 \sigma^2 [G(\vec{x},z,0;\vec{x},z,0) - G(\vec{x},z,0;-\vec{x},z,0)]\}\,. \quad (18)$$

The first term is the shot noise contribution and, by simple inspection of Fig. 2(c), one sees that the expression between square brackets is negative, in the far field, because the peak of G for $\vec{x}' = -\vec{x}$ is much higher than that for $\vec{x}' = \vec{x}$. Therefore the fluctuations of ΔI are *below shot noise*, which is a *nonclassical squeezing effect.* Conversely, in the case of a classical field the fluctuations are necessarily above shot noise, hence $G(\vec{x},z,0;\vec{x},z,0) > G(\vec{x},z,0;-\vec{x},z,0)$, i.e., no classical field can exhibit a far field intensity correlation function with the shape of Figs. 2(c) or 3(b) [11].

The amount of squeezing in Eq. (18) is quantitatively irrelevant, because the shot noise is larger than the rest by a factor $[\gamma \Delta t \sigma / w(z)^2]^{-1} \ll 1$. In order to obtain a significant squeezing effect, we must consider the spectrum of the fluctuations of the intensity difference,

$$V(\vec{x},z,\omega) = \int_{-\infty}^{+\infty} dt e^{-i\omega t} \langle I_-(\vec{x},z,t) I_-(\vec{x},z,0)\rangle\,, \quad (19)$$

which is linked to $\tilde{G}$; in addition, the regions $R(\vec{x})$ and $R(-\vec{x})$ must be selected in such a way that they encompass the entire peaks of $\tilde{G}$ [for the case of Fig. 3, the regions are shown in Fig. 4(b)]. For the parameters of Fig. 3, i.e., $\Delta_{00} = -0.5$, $\eta/\gamma = 0.1$, $\mathcal{A}_P = 0.5$ (the threshold is $\mathcal{A}_P = 1$, for $\Delta_{00} \leq 0$), and for $\omega = 0$, we obtained a quantum noise reduction in V of the order of 75% below shot noise. Closer to threshold ($\mathcal{A}_P = 0.9$), this value reduces to 70%. These figures improve further when η/γ is decreased, i.e., when mirror curvature decreases; e.g., for $\eta/\gamma = 0.05$ we obtained 82% quantum noise reduction for $\mathcal{A}_P = 0.5$ and 79% for $\mathcal{A}_P = 0.9$. This arises from the fact that by decreasing η/γ the far field peaks of $\tilde{G}$ become narrower and higher, and the peak at $\vec{x}' = -\vec{x}$ becomes more dominant with respect to the peak at $\vec{x}' = \vec{x}$.

We note that the squeezing in the intensity difference I_- has a *local* character, and therefore corresponds to a new kind of nonclassical state. The familiar squeezing properties refer to the beam as a whole, whereas here we consider portions of the beam, which can be taken smaller and smaller as η/γ is decreased. Our results demonstrate that there is a definite quantum correlation between the points of the transverse plane opposite with respect to the axis of the system. They hold also in the case of a quasiconcentric cavity.

In conclusion, we have shown that the far field configuration shown in Figs. 2(c) and 3(d) carries a precise quantum signature, and provides emphatic spatial evidence of the twin photon emission in the OPO. Our figures refer to the correlation function of the intensity fluctuations, but similar results can be obtained by considering a balanced homodyne detection [12] instead of a direct detection of the signal field. In this case, one observes the quantity $\{\exp(-i\theta) A_{\rm out}(\vec{x},z,t) + \text{H.c.}\}$, where θ is the phase of the local oscillator. Considering the total number of photons $N(\vec{x})$ which cross a finite region $R(\vec{x})$ in a homodyne detection scheme, we found that, for an appropriate local oscillator phase $\overline{\theta}$, the fluctuations in the difference $N(\vec{x}) - N(-\vec{x})$ are below shot noise, and the same holds true for the sum $N(\vec{x}) + N(-\vec{x})$ when $\theta = \overline{\theta} + \pi/2$. On the basis of these results, which will be discussed in a future publication, we are presently investigating the existence of a precise EPR paradox for continuous variables in this system, which would correspond to an even stronger quantum signature.

We thank C. Fabre and S. Schiller for very stimulating discussions. Research done in the framework of the Networks "Nonclassical Light" and "Quantum Structures" of the DGXII. of the European Union.

*Present address: Abteilung für Quantenphysik, Universität Ulm, Albert-Einstein-Allee 11, D-89069 Ulm, Germany.

[1] D. C. Burnham and D. L. Weinberg, Phys. Rev. Lett. **25**, 84 (1970); S. R. Friberg, C. H. Hong, and L. Mandel, Phys. Rev. Lett. **54**, 2011 (1985).
[2] H. Heidmann, R. J. Horowicz, E. Giacobino, and C. Fabre, Phys. Rev. Lett. **59**, 2555 (1987).
[3] O. Aytur and P. Kumar, Phys. Rev. Lett. **65**, 1551 (1990).
[4] P. G. Kwiat, K. Mattle, H. Weinfurter, A. Zeilinger, A. V. Sergienko, and Y. Shih, Phys. Rev. Lett. **75**, 4337 (1995).
[5] M. P. Reid and P. D. Drummond, Phys. Rev. Lett. **60**, 2731 (1988); Z. Y. Ou, S. F. Pereira, H. J. Kimble, and K. C. Peng, Phys. Rev. Lett. **68**, 3663 (1992).
[6] A. Gatti and L. A. Lugiato, Phys. Rev. A **52**, 1675 (1995); A. Gatti, H. Wiedemann, L. A. Lugiato, I. Marzoli, G. L. Oppo, and S. M. Barnett (to be published).
[7] L. A. Lugiato and I. Marzoli, Phys. Rev. A **52**, 4886 (1995).
[8] L. A. Lugiato and G. Grynberg, Europhys. Lett. **29**, 678 (1995).
[9] A. Yariv, *Quantum Electronics* (Wiley, New York, 1989), 3rd ed., pp. 136–154.
[10] C. W. Gardiner, *Quantum Noise* (Springer, Berlin, 1994).
[11] A measurement of the intensity correlation function in the far field has been reported in A. Maitre, A. Petrossian, A. Blouin, M. Pinard, and G. Grynberg, Opt. Commun. **116**, 153 (1995).
[12] D. F. Walls and G. J. Milburn, *Quantum Optics* (Springer, Berlin, 1994).